Article

Elucidation of the Thermochemical Properties of Triphenyl- or Tributyl-Substituted Si-, Ge-, and Sn-Centered Radicals by Means of Electrochemical Approaches and Computations

Allan Hjarbk Holm, Tore Brinck, and Kim Daasbjerg

J. Am. Chem. Soc., **2005**, 127 (8), 2677-2685• DOI: 10.1021/ja044687p • Publication Date (Web): 03 February 2005

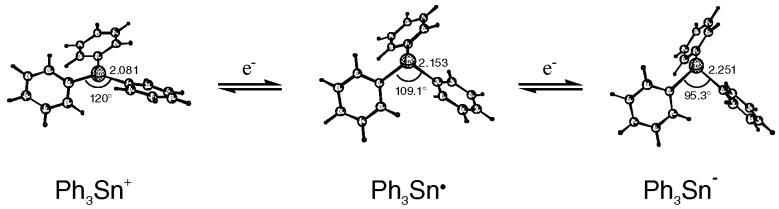

More About This Article

Additional resources and features associated with this article are available within the HTML version:

- Supporting Information
- Links to the 1 articles that cite this article, as of the time of this article download
- Access to high resolution figures
- Links to articles and content related to this article
- Copyright permission to reproduce figures and/or text from this article

View the Full Text HTML

J|A|C|S
ARTICLES
Published on Web 02/03/2005

Elucidation of the Thermochemical Properties of Triphenyl- or Tributyl-Substituted Si-, Ge-, and Sn-Centered Radicals by Means of Electrochemical Approaches and Computations

Allan Hjarbæk Holm,[¶] Tore Brinck,*[,#] and Kim Daasbjerg*[,¶]

Contribution from the Department of Chemistry, University of Aarhus, Langelandsgade 140, DK-8000 Aarhus C, Denmark, and Department of Physical Chemistry, Royal Institute of Technology, SE-10044 Stockholm, Sweden

Received September 2, 2004; E-mail: kdaa@chem.au.dk (K.D.); tore@physchem.kth.se (T.B.)

Abstract: Redox potentials of a number of triphenyl- or tributyl-substituted Si-, Ge-, or Sn-centered radicals, $R_3M^{\bullet}$, have been measured in acetonitrile, tetrahydrofuran, or dimethyl sulfoxide by photomodulated voltammetry or through a study of the oxidation process of the corresponding anions in linear sweep voltammetry. For the results pertaining to the $Ph_3M^{\bullet}$ series (including literature data for M = C), the order of reduction potentials follows Sn > Ge > C > Si, while for the two oxidation potentials, it is C > Si. The effect of the R group on the redox properties of $R_3Sn^{\bullet}$ is pronounced in that the reduction potential is more negative by 490 mV in tetrahydrofuran (390 mV in dimethyl sulfoxide) when R is a butyl rather than a phenyl group. The experimental trends have been substantiated through quantum chemical calculations, and they can be explained qualitatively by considering a combination of effects, such as charge capacity being most pronounced for the heavier elements, resonance stabilization present for the planar $Ph_3C^{\bullet}$ and all R_3M^{+}, and finally a contribution from solvation. The solvation of R_3M^{-} is observed to be relatively strong because of a rather localized negative charge in the pyramidal geometry. However, there is no evidence in the calculations to support the existence of covalent interactions between solvent and anions. The solvation of R_3M^{+} is relatively weak, which may be attributed to the planar geometry around the center atom, leading to more spread out charge than that for a pyramidal geometry. Although the calculated solvation energies based on the polarizable continuum model approach exhibit the expected trends, they are not able to reproduce the experimentally derived values on a detailed level for these types of ions. An evaluation of the general performance of the continuum model is provided on the basis of present and previous studies.

Introduction

Chemical compounds containing Si, Ge, or Sn atoms have attracted considerable attention due to their potential in the development of new types of materials displaying excellent pattern transfer[1] and photoconducting properties.[2,3] Recently, synthesis of polygermanes and polysilanes by electrochemical means has been reported,[4−6] making the knowledge of the redox potentials of the species involved essential for predicting and ultimately adjusting whether a radical or ionic pathway should be followed. In the literature, only few reports have been concerned with the estimation of the potentials of these types of radicals, even if a radical, such as $Bu_3Sn^{\bullet}$, has found widespread applications in synthesis.[7] Tanner et al. applied photomodulated voltammetry in the study of $Ph_3Sn^{\bullet}$ and $Bu_3Sn^{\bullet}$,[8] but the investigations were difficult because of experimental limitations.

The primary objective of the present paper is to characterize the redox properties of Si-, Ge-, and Sn-centered radicals in order to gain insight into the fundamental thermochemical properties of group IV elements by evaluating the effect of size and electron configuration. Ultimately, this may also provide useful guidelines for controlling polymerization processes involving these types of species. As chemical objects, we selected the three radicals, $Ph_3M^{\bullet}$ (M = Si, Ge, or Sn), as they with their comparatively high steric hindrance and delocalization features should present relatively fewest problems in electrochemical experiments with respect to adsorption and sluggish charge transfers. Included in the study was also $Bu_3Sn^{\bullet}$ to assess the group effect on the central atom and at the same time

[¶] University of Aarhus.
[#] Royal Institute of Technology.

(1) Hayase, S.; Nakano, Y.; Yoshikawa, S.; Ohta, H.; Sato, Y.; Shiobara, E.; Miyoshi, S.; Onishi, Y.; Abe, M.; Matsuyama, H.; Ohiwa, Y. *Chem. Mater.* **2001**, *13*, 2186.
(2) West, R.; David, L. D.; Djurovich, P. I.; Stearley, K. L.; Srinivasan, K. S. V.; Yu, H. *J. Am. Chem. Soc.* **1981**, *103*, 7352. (b) Miller, R. D. *Angew. Chem., Int. Ed. Engl.* **1989**, *28*, 1733.
(3) Matsukawa, K.; Tamai, T.; Inoue, H. *Appl. Phys. Lett.* **2000**, *77*, 675. (b) Ostapenko, N. I.; Sekirin, I. V.; Tulchynskaya, D. N.; Suto, S.; Watanabe, A. *Synth. Met.* **2002**, *129*, 19.
(4) Ishifune, M.; Kashimura, S.; Kogai, Y.; Fukuhara, Y.; Kato, T.; Bu, H.-B.; Yamashita, N.; Murai, Y.; Murase, H.; Nishida, R. *J. Organomet. Chem.* **2000**, *611*, 26. (b) Kashimura, S.; Ishifune, M.; Yamashita, N.; Bu, H.-B.; Takebayashi, M.; Kitajima, S.; Yoshihara, D.; Kataoka, Y.; Nishida, R.; Kawasaki, S.; Murase, H.; Shono, T. *J. Org. Chem.* **1999**, *64*, 6615.
(5) Okano, M.; Watanabe, K.; Totsuka, S. *Electrochemistry* **2003**, *71*, 257.
(6) Subramanian, K. *J. Macromol. Sci., Rev. Macromol. Chem. Phys.* **1998**, *C38* (4), 637.
(7) Chatgilialoglu, C. In *Radicals in Organic Synthesis*; Renaud, P., Sibi, M. P., Eds.; Wiley: Weinheim, Germany, 2001; p 28.
(8) Tanner, D. D.; Harrison, D. J.; Chen, J.; Kharrat, A.; Wayner, D. D. M.; Griller, D.; McPhee, D. J. *J. Org. Chem.* **1990**, *55*, 3321.

Scheme 1. Generalized Electrode Processes (M = Si, Ge, or Sn, and R = Ph or Bu)

$$R_3M^+ \underset{}{\overset{e,\ E^\circ_{R_3M^+/R_3M^\bullet}}{\rightleftharpoons}} R_3M^\bullet \overset{e,\ E^\circ_{R_3M^\bullet/R_3M^-}}{\rightleftharpoons} R_3M^-$$

characterize one of the most commonly used radicals within the synthetic community.[7] Scheme 1 illustrates the generalized electrode processes under investigation.

The experimental strategy was based on the utilization of two independent electrochemical techniques, photomodulated voltammetry (PMV) and linear sweep voltammetry (LSV), to overcome the experimental difficulties encountered and to establish confidence in the results obtained. At the same time, quantum chemical calculations were carried out in order to obtain complementary information about the structure, the extent of electron delocalization, ionization potentials, electron affinities, and solvation energies. An interesting aspect of the last set of values is that they may be compared directly with experimentally derived solvation energies extracted from the measured potentials. In this manner, we have shown recently that continuum-based solvation models, in which the solvent is characterized solely by its dielectric constant, were adequate for predicting solvation energies of many organic anions, including carbanions,[9] thiophenoxides,[10,11] and arylselenoates.[12] On the other hand, quite severe deviations were seen for arylsulfenium[10,11] and arylselanylium cations[12] as the calculated values underestimated the absolute solvation energies by as much as 20−30 kcal mol^{-1}. We attributed this discrepancy to the presence of strong covalent bond formation between the solvent (i.e., acetonitrile) and the cation center. Indeed, the observed differences could be accounted for by incorporating such an adduct in the theoretical calculations using a supermolecular approach. An interesting issue, therefore, is whether the same sort of interaction would be present for the Ph_3M^+ studied herein.

Experimental Section

Materials. All investigated substrates were commercial and used in the highest grade available without further purification. Acetonitrile (MeCN) and tetrahydrofuran (THF) were obtained from Lab-Scan. MeCN was dried through a column of activated alumina, while THF was distilled over sodium and benzophenone. Dimethyl sulfoxide (DMSO, sure seal bottle) was purchased from Aldrich and used as received. The supporting electrolytes, tetrabutylammonium perchlorate (Bu_4NClO_4) and tetrabutylammonium tetrafluoroborate (Bu_4NBF_4), were prepared and purified by standard procedures.

Apparatus. The instrumental setup used in the photomodulated voltammetry technique has been described in detail recently.[9,10,12] It consisted of a 100 W Hg−Xe lamp (L8029, Hamamatsu) for generating radicals photolytically, a water filter, a chopper (651, EG&G Instruments), a lock-in amplifier (SR810 DSP, Stanford Research Systems), and a home-built electrochemical flow-cell for detecting the radicals. As working electrode, a net made of carbon fibers (Grafil 34, Grafil Inc.) or a gold mini-grid (1000 mesh, Dansk Hollandsk Ædelmetal) was used. A small platinum rod positioned in the outlet of the electrochemical cell served as counter electrode. The reference electrode was a Flex-Ref electrode purchased from World Precision Instruments.

In the linear sweep experiments, a $\phi = 0.68$ or 1 mm glassy carbon (Sigradur G, HTW) disk was employed as working electrode. The electrode surface was carefully polished before each experiment with a 0.25 μm diamond suspension and rinsed in ethanol. The counter electrode was a platinum coil melted into glass, while a silver wire in the solvent system separated from the solution by a ceramic disk served as quasi-reference electrode. The ohmic drop in both the LSV and PMV experiments was compensated with a positive feedback system incorporated in the home-built potentiostat.

Procedure. The primary advantage of the PMV technique is that under optimal conditions, it allows the simultaneous determination of the half-wave oxidation and reduction potentials, $E^{ox}_{1/2}$ and $E^{red}_{1/2}$, of photolytically generated radicals by recording the current as a function of the electrode potential.[13] Because the photolyzing light is modulated with a certain frequency, a phase-sensitive detection of the current that will be modulated with the very same frequency will result in a substantial increase in the signal/noise ratio, allowing the recording of voltammograms for reactive radicals even in submicromolar concentrations. The most direct approach for generating $R_3M^\bullet$ (M = Si, Ge, or Sn; R = Ph or Bu) consists of photolyzing the pertinent hexaphenyl or hexabutyl compounds, $(R_3M-)_2$, as shown in eq 1.

$$(R_3M-)_2 \xrightarrow{h\nu} 2\ R_3M^\bullet \qquad (1)$$

In most cases, however, this approach for promoting the homolytic bond cleavage cannot be used as the center σ bond in $(Ph_3M-)_2$ is quite strong, having bond dissociation energies ranging from 45 (M = Sn) to 63 (M = Ge) and 78 kcal mol^{-1} (M = Si).[14] In addition, the solubility of $(Ph_3M-)_2$ is low in MeCN, which is the preferred solvent for this kind of measurement because of its relatively low reactivity toward radicals. In the study of $(Ph_3Sn-)_2$, we therefore had to resort to THF. An alternative and indirect approach was also considered, in which *tert*-butoxyl radicals were generated by photolyzing di-*tert*-butyl peroxide (eq 2), followed by hydrogen abstraction from R_3MH (eq 3).

$$(tert\text{-}BuO-)_2 \xrightarrow{h\nu} 2\ tert\text{-}BuO^\bullet \qquad (2)$$

$$R_3MH + tert\text{-}BuO^\bullet \longrightarrow R_3M^\bullet + tert\text{-}BuOH \qquad (3)$$

The latter reaction is very efficient, proceeding by a rate constant as high as 3.5×10^8 M^{-1} s^{-1} in the case of Bu_3SnH (in benzene).[15]

The substrate concentration used was 2−500 mM in deaerated THF or MeCN containing supporting electrolyte, and in the case of the second photolytic approach (i.e., eqs 2 and 3) 10 vol % di-*tert*-butyl peroxide. Samples were allowed to flow through the cell at a rate of 2−3 mL min^{-1} in order to prevent depletion of substrate and product accumulation. The chopping frequency and sweep rate employed throughout the study were 134 Hz and 0.1 V s^{-1}, respectively.[16] The voltammograms were corrected for the background current recorded in the absence of substrate. All half-wave potentials were measured relative to the standard potential of the ferrocenium/ferrocene (Fc^+/Fc) redox couple and converted to SCE by employing the standard potentials of 0.410 V versus SCE in MeCN and 0.570 V versus SCE in THF determined for Fc^+/Fc elsewhere.[17]

(9) Brinck, T.; Larsen, A. G.; Madsen, K. M.; Daasbjerg, K. *J. Phys. Chem. B* **2000**, *104*, 9887.
(10) Larsen, A. G.; Holm, A. H.; Roberson, M.; Daasbjerg, K. *J. Am. Chem. Soc.* **2001**, *123*, 1723.
(11) Brinck, T.; Carlqvist, P.; Holm, A. H.; Daasbjerg, K. *J. Phys. Chem. A* **2002**, *106*, 8827.
(12) Holm, A. H.; Yusta, L.; Carlqvist, P.; Brinck, T.; Daasbjerg, K. *J. Am. Chem. Soc.* **2003**, *125*, 2148.
(13) Wayner, D. D. M.; Griller, D. *J. Am. Chem. Soc.* **1985**, *107*, 7764. (b) Wayner, D. D. M.; McPhee, D. J.; Griller, D. *J. Am. Chem. Soc.* **1988**, *110*, 132.
(14) Saiful, I. S. M.; Ohba, Y.; Mochida, K.; Yamauchi, S. *Phys. Chem. Chem. Phys.* **2001**, *3*, 1011.
(15) Shaw, W. J.; Kandandarachchi, P.; Franz, J. A.; Autrey, T. *Organometallics* **2004**, *23*, 2080.
(16) No significant changes were observed to the measured half-wave potentials upon varying the frequency. For a discussion of the theoretical aspects of the PMV technique, see: Nagaoka, T.; Griller, D.; Wayner, D. D. M. *J. Phys. Chem. Soc.* **1991**, *95*, 6264.
(17) Daasbjerg, K.; Pedersen, S. U.; Lund, H. In *General Aspects in the Chemistry of Radicals*; Alfassi, Z. B., Ed.; Wiley: Chichester, U.K., 1999; Chapter 12, p 410.

In LSV, the oxidation process of R_3M^- was studied in the sweep rate range of 0.1−20 V s^{-1} in order to characterize the $R_3M^{\bullet}/R_3M^-$ couple.[18] The anions were generated in concentrations of 1−2 mM through a deprotonation of the pertinent hydrides using the potassium salt of dimsyl, $CH_3S(O)CH_2^-K^+$, as base in 0.1 M Bu_4NClO_4/DMSO (eq 4).[19]

$$R_3MH + CH_3S(O)CH_2^-K^+ \longrightarrow R_3M^-K^+ + CH_3S(O)CH_3 \quad (4)$$

In MeCN, the deprotonation could only be accomplished successfully for Ph_3SnH. All solutions were carefully deaerated with argon before use. Digital simulations were carried out using the DigiSim version 3.03 software.[20] The transfer coefficient, α, was set equal to 0.5, and the diffusion coefficient, *D*, was assumed to be 10^{-5} cm^2 s^{-1} for all species involved. All potentials were converted to SCE by measuring them relative to the standard potential of Fc^+/Fc (0.430 V versus SCE in DMSO).[17]

Theoretical Approach. Optimized geometries, harmonic vibrational frequencies, and energies for all molecules have been computed using Kohn−Sham density functional theory with the B3LYP[21,22] correlation-exchange functional in Gaussian 98.[23] The LanL2DZ basis set, which describes the inner electrons of elements heavier than neon by an effective core potential, was utilized in the calculations.[24] This basis set was augmented by d-functions on non-hydrogen atoms and diffuse p-functions on the central C, Si, Ge, and Sn elements.[25] It is well-known that diffuse functions are necessary to obtain accurate energetics for processes involving anions. Therefore, electron affinities were calculated from single point energies obtained with a basis set that in addition to d-functions was augmented with diffuse p-functions on all non-hydrogen atoms. The exponents of these functions were in all cases taken from the work of Check et al.[25]

Solvation energies have been calculated at the B3LYP level using the recent implementation of the polarizable continuum model (PCM)[26] in Gaussian 98.[23] The same basis sets were used as in the geometry optimizations. The solute cavities in the calculations were made up of overlapping spheres centered at the atomic nuclei. The radii of these spheres were taken as the van der Waals radii of Bondi,[27] as implemented in Gaussian 98, and scaled by an appropriate factor. A scale factor of 1.2 has been found to be suitable for computation of hydration free energies of organic molecules.[28] This is also the default scale factor in Gaussian 98. However, because the use of this factor led to numerical problems in the PCM computations for some of the molecules studied herein, we choose to employ a larger scale factor of 1.3 throughout the study. The larger scale factor generally led to an increase in the solvation energy by 2−4 kcal mol^{-1} for the ionic compounds. Much smaller changes were observed for neutral radicals. The solvent parameters, including the dielectric constant (36.64), were the same as those implemented for MeCN in the program, although it should be noted that the influence of the exact value of the dielectric constant was found to be rather modest.

Spin densities and atomic charges have been computed using Mulliken population analysis.[29] Since this method has been criticized for being very basis set-dependent and sometimes leading to unrealistic results,[30] we have also computed charges using the CHELPG approach.[31] In this latter method, the charges are fitted to reproduce the computed electrostatic potential of the molecule. The electrostatic potential (ESP) is a real physical property, and its calculation is not dependent on the use of a basis set. However, a problem associated with ESP charge derivations is that charges of atoms buried inside the molecule are not always well-defined.[32] All quantum chemical calculations were performed using the Gaussian 98 suite of programs.

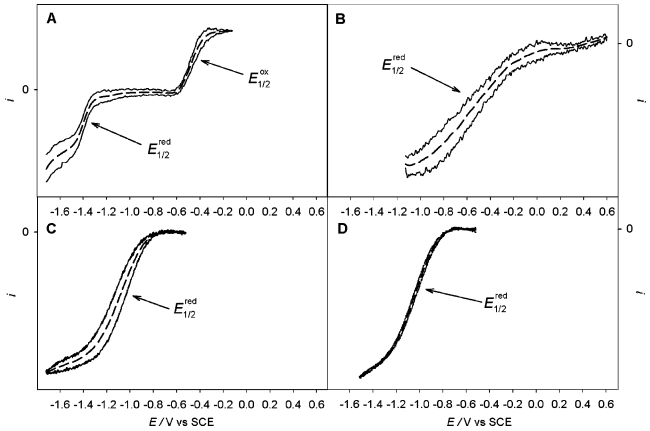

Figure 1. Photomodulated voltammograms of (A) $Ph_3Si^{\bullet}$ generated by photolysis of 10 vol % (*tert*-BuO−)$_2$ + 0.5 M Ph_3SiH in 0.1 M Bu_4NClO_4/MeCN at a gold mini-grid electrode; (B) $Ph_3Sn^{\bullet}$ generated by photolysis of 0.025 M $(Ph_3Sn-)_2$ in 0.3 M Bu_4NBF_4/THF at a carbon fiber net; (C) $Bu_3Sn^{\bullet}$ generated by photolysis of 0.02 M $(Bu_3Sn-)_2$ in 0.3 M Bu_4NBF_4/THF at a gold mini-grid electrode; and (D) $Bu_3Sn^{\bullet}$ generated by photolysis of 10 vol % (*tert*-BuO−)$_2$ + 0.02 M Bu_3SnH in 0.1 M Bu_4NClO_4/MeCN at a gold mini-grid electrode. All voltammograms were recorded at a sweep rate of 0.1 V s^{-1} and corrected for the background current. Signal average of forward and backward sweeps is shown by the dashed curves (- - -).

Results and Discussions

Photomodulated Voltammetry. Figure 1A shows a typical photomodulated voltammogram recorded for $Ph_3Si^{\bullet}$. Both an oxidation and a reduction wave are seen corresponding to the generalized processes depicted in Scheme 1. It is noteworthy that there is not complete coincidence of the forward and reverse sweeps, and that the wave widths, $|E_{3/4} - E_{1/4}|$, of 120 and 110 mV, respectively, are larger than the value of 56.4 mV expected for a nernstian process unaffected by preceding or follow-up chemistry.[33] Furthermore, it was found in separate experiments that the half-wave potentials, $E_{1/2}^{ox}$ (−0.41 V versus SCE) and

(18) Note that the $R_3M^+/R_3M^{\bullet}$ couple cannot be studied in a similar manner since the stability of the R_3M^+ precursor would be too low.
(19) Olmstead, W. N.; Margolin, Z.; Bordwell, F. G. *J. Org. Chem.* **1980**, *45*, 3295.
(20) Rudolph, M.; Feldberg, S. W. *DigiSim*, version 3.03; Bioanalytical Systems, Inc.: West Lafayette, IN.
(21) Becke, A. D. *J. Chem. Phys.* **1993**, *98*, 5648.
(22) Stephens, P. J.; Devlin, F. J.; Chablovski, C. F.; Frisch, M. J. *J. Phys. Chem.* **1994**, *98*, 11623.
(23) Frisch, M. J.; Trucks, G. W.; Schlegel, H. B.; Scuseria, G. E.; Robb, M. A.; Cheeseman, J. R.; Zakrzewski, V. G.; Montgomery, J. A.; Stratmann, E.; Burant, J. C.; Dapprich, S.; Millam, J. M.; Daniels, A. D.; Kudin, K. N.; Strain, M. C.; Farkas, O.; Tomasi, J.; Barone, V.; Cossi, M.; Cammi, R.; Mennucci, B.; Pomelli, C.; Adamo, C.; Clifford, S.; Ochterski, J.; Petersson, G. A.; Ayala, P. Y.; Cui, Q.; Morokuma, K.; Malick, D. K.; Rabuck, A. D.; Raghavachari, K.; Foresman, J. B.; Cioslowski, J.; Ortiz, J. V.; Baboul, A. G.; Stefanov, B. B.; Liu, G.; Liashenko, A.; Piskorz, P.; Komaromi, I.; Gomperts, R.; Martin, R. L.; Fox, D. J.; Keith, T.; Al-Laham, M. A.; Peng, C. Y.; Nanayakkara, A.; Gonzalez, C.; Challacombe, M.; Gill, P. M. W.; Johnson, B.; Chen, W.; Wong, M. W.; Andres, J. L.; Head-Gordon, M.; Replogle, E. S.; Pople, J. A. *Gaussian 98*, revision A.7; Gaussian, Inc.: Pittsburgh, PA, 1998.
(24) Hay, P. J.; Wadt, W. R. *J. Chem. Phys.* **1985**, *82*, 270. (b) Hay, P. J.; Wadt, W. R. *J. Chem. Phys.* **1985**, *82*, 284. (c) Hay, P. J.; Wadt, W. R. *J. Chem. Phys.* **1985**, *82*, 299.
(25) Check, C. E.; Faust, T. O.; Bailey, J. M.; Wright, B. J.; Gilbert, T. M.; Sunderlin, L. S. *J. Phys. Chem.* A **2001**, *105*, 8111.
(26) Cossi, M.; Barone, V.; Cammi, R.; Tomasi, J. *Chem. Phys. Lett.* **1996**, *255*, 327.
(27) Bondi, A. *J. Phys. Chem.* **1964**, *68*, 441.
(28) Tomasi, J.; Persico, M. *Chem. Rev.* **1994**, *94*, 2027.
(29) Mulliken, R. S. *J. Chem. Phys.* **1955**, *23*, 1833.
(30) Politzer, P.; Harris, R. R. *J. Am. Chem. Soc.* **1970**, *92*, 6451. (b) Reed, A. E.; Weinstock, R. B.; Weinhold, F. J. *Chem. Phys.* **1985**, *83*, 735. (c) Williams, D. E. In *Reviews in ComputationaI Chemistry*; Lipkowitz, K. B., Boyd, D. B., Eds.; VCH Publishers: New York, 1991; Vol. 2, p 431.
(31) Breneman, C. M.; Wiberg, K. B. *J. Comput. Chem.* **1990**, *11*, 361.
(32) Cornell, W. D.; Cieplak, P.; Bayly, C. I.; Kollman, P. A. *J. Am. Chem. Soc.* **1993**, *115*, 9620.
(33) Bard, A. J.; Faulkner, L. R. *Electrochemical Methods: Fundamentals and Applications*; Wiley: New York, 2001.

$E^{red}_{1/2}$ (−1.39 V versus SCE), determined as an average of the forward and reverse sweeps, were independent of electrode material and sweep number, indicating that adsorption is not a crucial factor. Usually the presence of broad waves is due to slow charge-transfer kinetics at the electrode surface, that is, quasi-reversible electrode processes, and consequently, the values of $E^{ox}_{1/2}$ and $E^{red}_{1/2}$ cannot a priori be set equal to the standard potentials, $E^{o}_{R_3M^+/R_3M^\bullet}$ and $E^{o}_{R_3M^\bullet/R_3M^-}$.[33] At the same time, there may be an effect on the position of the waves from fast homogeneous reactions involving R_3M^+ and $R_3M^\bullet$. While R_3M^- has a high stability in aprotic solvents, $R_3M^\bullet$ is expected to dimerize in a fast process and the strong electrophile, R_3M^+, would react with any nucleophile present in the solution, be it residual water or the solvent itself.[34] These effects are difficult to estimate quantitatively, but on account of the similar wave shapes observed in our PMV studies on arylthiyl,[10] arylselanyl,[12] and α-hydroxyalkyl radicals,[35] and the analysis given therein, we expect the half-wave potentials to be within 100 mV of the corresponding standard potentials.

For $Ph_3Ge^\bullet$, none of the two approaches in the PMV method gave reliable results, presumably because the relatively strong σ bonds in $(Ph_3Ge—)_2$ and $Ph_3Ge—H$ made it difficult to generate the radical in sufficiently high concentrations.[14] In that respect, the PMV approach worked much better for $Ph_3Sn^\bullet$ and $Bu_3Sn^\bullet$, as illustrated in Figure 1B−D. The voltammogram for $Ph_3Sn^\bullet$ is characterized by the appearance of a broad reduction wave with $E^{red}_{1/2} = -0.51$ V versus SCE and $|E_{3/4} - E_{1/4}| \approx 260$ mV, while no oxidation wave is observable. The large width of the wave seriously questions the thermodynamic significance of such a result. For $Bu_3Sn^\bullet$, it is possible to observe the reduction process using both approaches in PMV, that is, direct photolysis of $(Bu_3Sn—)_2$ in THF (eq 1) and the indirect hydrogen abstraction method involving Bu_3SnH in MeCN (eqs 2 and 3). The coincidence of the forward and reverse sweeps is poorer for the first approach in THF (Figure 1C), but the average value of $E^{red}_{1/2}$ for the two sweeps is not affected and remains constant, independent of the sweep number. The measured $E^{red}_{1/2}$ is −1.00 V versus SCE for the first approach in THF and −1.12 V versus SCE for the second approach in MeCN. As to the oxidation process, it was not possible to obtain anything but poorly reproducible waves. The explanation probably relies on adsorption phenomena as also noted by Tanner et al.[8] Experiments were performed with a variety of changes to the setup, different electrode materials (gold, platinum, or carbon), supporting electrolytes (Bu_4NClO_4 or Bu_4NBF_4), solvents (THF or MeCN), and concentrations, but with no success. Thus, only a rough estimate of $E^{ox}_{1/2} = 0.20$ V versus SCE for $Bu_3Sn^\bullet$ in MeCN can be provided.

Linear Sweep Voltammetry. In LSV, the oxidation process of R_3M^- generated from eq 4 was studied in order to characterize the $R_3M^\bullet/R_3M^-$ couples and, in this manner, judge the thermodynamic significance of the $E^{red}_{1/2}$ values obtained in the PMV approach. In Figure 2, we have collected voltammograms for Ph_3Ge^-, Ph_3Sn^-, and Bu_3Sn^- recorded at a sweep rate, ν, of 0.5 V s^{-1} in DMSO; the measurements pertaining to Ph_3Si^- had to be abandoned because of low reproducibility. In all three cases, a characteristic irreversible one-electron oxidation

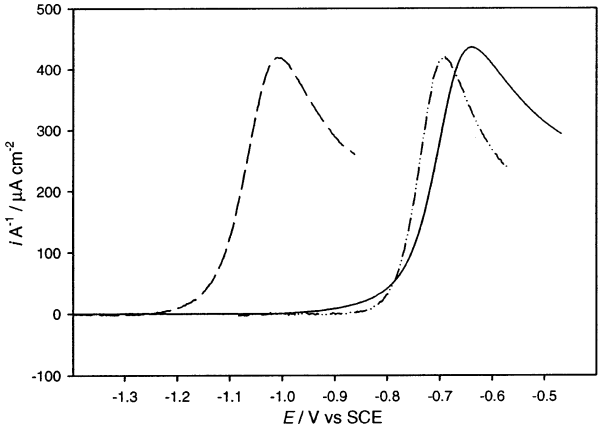

Figure 2. Linear sweep voltammograms of the oxidation of 1.2 mM Bu_3Sn^- (- - -), Ph_3Ge^- (−••−), and Ph_3Sn^- (—) in 0.1 M Bu_4NClO_4/DMSO at a glassy carbon electrode. Sweep rate = 0.5 V s^{-1}. The current is normalized with respect to the electrode area.

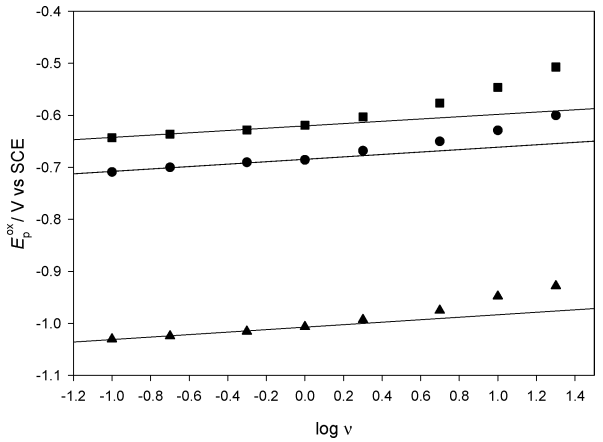

Figure 3. Plots of E^{ox}_p versus log ν for the oxidation of 1.2 mM Bu_3Sn^- (▲), Ph_3Ge^- (●), and Ph_3Sn^- (■) in 0.1 M Bu_4NClO_4/DMSO at a glassy carbon electrode. Sweep rates applied are in the range of 0.1−20 V s^{-1}, but only the four points pertaining to 0.1−1 V s^{-1} are included in the linear regression analysis.

wave appears with the peak potential, E^{ox}_p, being in the range from −1.0 to −0.65 V versus SCE.[36] To elucidate the mechanism, E^{ox}_p was measured as a function of log ν. As seen in Figure 3, the linear dependence observable at low ν in the range of 0.1−1 V s^{-1} is replaced by distinct curvature at higher ν. The slopes of 20 ± 3 mV $decade^{-1}$ found for the linear parts ($r^2 > 0.95$) are in fair agreement with the 19.7 mV $decade^{-1}$ expected for a rapid electron transfer (eq 5) followed by a fast dimerization reaction (eq 6), formally described as an E_rC_2 mechanism.[33]

$$R_3M^- - e \rightleftarrows R_3M^\bullet \quad (5)$$

$$2R_3M^\bullet \xrightarrow{k_d} (R_3M—)_2 \quad (6)$$

As long as the kinetic control is fully by eq 6, that is, when $\nu \leq 1$ V s^{-1}, the relationship between E^{ox}_p and the standard potential $E^{o}_{R_3M^\bullet/R_3M^-}$ is given by eq 7.[37,38]

(34) In practice, the effect of adding nucleophiles has been found to be small in the PMV approach; see ref 10.
(35) Lund, T.; Wayner, D. D. M.; Jonsson, M.; Larsen, A. G.; Daasbjerg, K. *J. Am. Chem. Soc.* **2001**, *123*, 12590.
(36) Note that the dimsyl anion, $CH_3S(O)CH_2^-K^+$, also gives rise to an oxidation peak in the same potential region. This peak could be "titrated" so that only the peak pertaining to the $R_3M^-/R_3M^\bullet$ couple was visible.
(37) Savéant, J.-M.; Vianello, E. *Electrochim. Acta* **1967**, *12*, 1545.

$$E_p^{ox} = 0.902\frac{RT}{F} + E^o_{R_3M^{\bullet}/R_3M^-} - \frac{RT}{3F}\ln\left(\frac{2k_dC^o}{\nu}\frac{2RT}{3F}\right) \quad (7)$$

In the above expression, $2k_d$ is the dimerization rate constant and C^o is the bulk concentration of R_3M^-. For $2k_d$, we use the value of 3.6×10^9 M^{-1} s^{-1} determined for $Bu_3Sn^{\bullet}$ by transient absorption spectroscopy in benzene.[15] Thus, we find that $E^o_{Ph_3Ge^{\bullet}/Ph_3Ge^-} = -0.61$ V versus SCE (DMSO), $E^o_{Ph_3Sn^{\bullet}/Ph_3Sn^-} = -0.46$ V versus SCE (MeCN), $E^o_{Ph_3Sn^{\bullet}/Ph_3Sn^-} = -0.54$ V versus SCE (DMSO), and $E^o_{Bu_3Sn^{\bullet}/Bu_3Sn^-} = -0.93$ V versus SCE (DMSO), with an estimated uncertainty of ± 0.05 V.[39]

The deviating points in the plot of E_p^{ox} versus log ν at large sweep rates show that the systems under these conditions no longer are under full kinetic control by eq 6 but rather that there is a mixed kinetic control by eqs 5 and 6.[40] In this regime, a rough estimation of the standard heterogeneous rate constant, $k°$, for the charge-transfer step in eq 5 can be determined on the basis of simulations of the voltammograms.[20] For all of the systems studied, we find a value of $k° \approx 0.02$ cm s^{-1}. Thus, the effect on $k°$ of substituting butyl with phenyl groups in the $R_3Sn^{\bullet}/R_3Sn^-$ couple is small, suggesting that the extent of delocalization in the phenyl moieties cannot be extensive.[41]

Table 1 summarizes the electrochemical data obtained for $Ph_3Si^{\bullet}$, $Ph_3Ge^{\bullet}$, $Ph_3Sn^{\bullet}$, and $Bu_3Sn^{\bullet}$. For comparison, we have included literature data for $Ph_3C^{\bullet}$ to have almost the complete series of group IV elements.[42] Even if experimental difficulties because of adsorption prevented some of the measurements, the consistency between the two sets of $E^{red}_{1/2}$ and $E^o_{R_3M^{\bullet}/R_3M^-}$ values available for $Ph_3Sn^{\bullet}$ and $Bu_3Sn^{\bullet}$ with variations of less than 50 and 190 mV (for different solvents), respectively, is acceptable. This coherence underlines the thermodynamic significance of the PMV results, despite the broad waves recorded. In a previous study, the same two Sn-centered radicals were investigated using PMV.[8] Although the authors did not place a great deal of confidence in the measured $E^{red}_{1/2}$ values of -0.59 V (THF) for $Ph_3Sn^{\bullet}$ and -1.13 V versus SCE (MeCN) and -1.29 V versus SCE (THF) for $Bu_3Sn^{\bullet}$, they are relatively close to the present results with the largest deviation of 290 mV seen in the latter case. The lower limit of -0.43 V versus SCE estimated for the oxidation potential of $Bu_3Sn^{\bullet}$ on the basis of Marcus theory[43] is well within the 0.20 V versus SCE determined for $E^{ox}_{1/2}$ herein. Because of the experimental challenges, we had to resort to the use of three different organic solvents, namely, MeCN, THF, and DMSO. However, the similarity of the reduction potentials obtained in the case of $Ph_3Sn^{\bullet}$ (within 80 mV) shows that the solvent effect is small. The same conclusion has been reached in studies pertaining to both localized and delocalized carbanions[9] and radical anions.[44]

On the basis of the measurements of potentials, we may now state that the electrochemical generation of polysilanes and polygermanes through an anionic polymerization route relies on the condition that the applied potentials should be more negative than approximately -1.4 and -0.6 V versus SCE, respectively, if the further reduction of the pertinent radicals to form the anions should be accomplished. For most precursors employed, this should present no problems.[4−6] Likewise, for the many important chain processes based on the active role of Sn-centered radicals,[7,45] it is important to ensure that the relevant potentials of any redox agents present are positioned in the range from -1 to 0.2 V versus SCE (in the case of $Bu_3Sn^{\bullet}$) if interference from reduction or oxidation processes should be avoided.

Before discussing the effect exerted by the different group IV elements on the potentials obtained, we will turn to a computation of geometries, charge distributions, ionization potentials, and electron affinities to get a better understanding of the essential features of the systems. These data are gathered in Tables 1 and 2.

Optimized Geometries and Computed Charge Distributions. Optimized geometries of $Ph_3Sn^{\bullet}$, $Bu_3Sn^{\bullet}$, and the corresponding ions are depicted in Figure 4. The structures of the remaining radicals and ions studied are available in the Supporting Information. Concerning the $Ph_3M^{\bullet}$ series, the geometry for the different elements exhibits distinct differences. While $Ph_3C^{\bullet}$ has a planar geometry around the central C atom, the heavier radicals are characterized by a pyramidal center. However, the pyramidal character increases gradually going down the periodic table; the C−M−C angle is 114.3, 112.0, and 109.1° for $Ph_3Si^{\bullet}$, $Ph_3Ge^{\bullet}$, and $Ph_3Sn^{\bullet}$, respectively. This suggests that π-resonance stabilization decreases in the same order. The gradual decrease can be explained by a decreasing C−M p-orbital overlap as the M atom gets heavier. The much stronger resonance interaction in $Ph_3C^{\bullet}$ compared to that of the other radicals is confirmed by the computed spin densities on the central atom. While the C atom has a spin density of 0.59, the heavier atoms all have densities around 0.8. These results do not support the decrease in resonance interaction going from Si to Sn suggested by the increasing pyramidality. However, such a discrepancy may be attributed to the known basis set dependency problem with the Mulliken population analysis.[46] A comparison of the computed properties for $Bu_3Sn^{\bullet}$ and $Ph_3Sn^{\bullet}$ reveals as expected that the C−Sn bond length as well as the spin density is larger for the former radical because of the lack of resonance interaction.

For the Ph_3M^+ series, all cations are predicted to be planar. At the same time, the C−M bond lengths are shorter than the

(38) Andrieux, C. P.; Nadjo, L.; Savéant, J.-M. *J. Electroanal. Chem.* **1973**, *42*, 223.

(39) The value of $2k_d = 3.6 \times 10^{10}$ M^{-1} s^{-1} determined in benzene is only slightly lower than the diffusion-controlled limit.[15] For our experiment carried out in acetonitrile, which is characterized by a higher limit of 4×10^{10} M^{-1} s^{-1} (Grampp, G.; Jaenicke, W. *Ber. Bunsen-Ges. Phys. Chem.* **1991**, *95*, 904), it is possible that $2k_d$ will be comparatively larger. In worst case, this might underestimate $E^o_{R_3M^{\bullet}/R_3M^-}$ by 20 mV. For the three experiments carried out in DMSO with a diffusion-controlled limit at 6×10^9 M^{-1} s^{-1}, the effect will be small.

(40) Andrieux, C. P.; Savéant, J.-M. Electrochemical Reactions. In *Investigations of Rates and Mechanisms of Reactions*, *Techniques of Chemistry*; Bernasconi, C. F., Ed.; Wiley: New York, 1986; Vol. VI/4E, Part 2, p 305.

(41) Although the estimated values of $k°$ imply that the electrode kinetics should be nernstian at the low sweep rates employed in PMV[16,33], the recorded waves were found to be relatively broad. However, as discussed in our previous studies on thiyl and selanyl radicals, there seems to be no simple correlation between $|E_{3/4} - E_{1/4}|$ and $k°$.[10,12]

(42) (a) Klein, E.; Rojahn, W. *Tetrahedron Lett.* **1969**, 2279. (b) Wasielewski, M. R.; Breslow, R. *J. Am. Chem. Soc.* **1976**, *98*, 4222.

(43) Eberson, L. *Electron Transfer Reactions in Organic Chemistry*; Springer-Verlag: Heidelberg, Germany, 1987.

(44) Shalev, H.; Evans, D. H. *J. Am. Chem. Soc.* **1989**, *111*, 2667.

(45) Tanaka, H.; Ogawa, H.; Suga, H.; Torii, S.; Jutand, A.; Aziz, S.; Suarez, A. G.; Amatore, C. *J. Org. Chem.* **1996**, *61*, 9402.

(46) That there indeed is an ambiguity involved in the partitioning of the electron density can be understood by comparing the charges obtained by Mulliken population analysis and the CHELPG approach. Both approaches show that $Ph_3C^{\bullet}$ has a significantly more negative central atom than the heavier $Ph_3M^{\bullet}$. However, the CHELPG charges are all negative, while the Mulliken charges are positive. In addition, the CHELPG charges become less negative going from Si to Sn, while the Mulliken charges show a more erratic behavior. The CHELPG charges support the expected decrease in resonance-donation to the center atom when going from Si to Sn.

Table 1. Half-Wave Potentials, $E^{red}_{1/2}$ and $E^{ox}_{1/2}$, and Standard Potentials, $E^{o}_{R_3M^{\bullet}/R_3M^-}$, Measured for $R_3M^{\bullet}$ at Carbon-Based or Gold Electrodes at 25 °C along with Computed Adiabatic Ionization Potentials (IP) and Electron Affinities (EA)

	$E^{ox}_{1/2}$ [a,b]	$\lvert E_{3/4} - E_{1/4}\rvert$ [c]	$E^{red}_{1/2}$ [a,b]	$\lvert E_{3/4} - E_{1/4}\rvert$ [c]	$E^{o}_{R_3M^{\bullet}/R_3M^-}$ [a,b]	IP[d]	EA[d]
$Ph_3C^{\bullet}$	0.27[e,f]				−0.97[e,g]	5.88	1.43 (1.56)[h]
$Ph_3Si^{\bullet}$	−0.41[e]	120	−1.39[e]	110		5.45	1.46
$Ph_3Ge^{\bullet}$					−0.61[i]	5.52	1.76
$Ph_3Sn^{\bullet}$			−0.51[j]	260	−0.54[i]−0.46[e]	5.67	2.08
$Bu_3Sn^{\bullet}$	(0.20)[e,k]	210	−1.12[e]−1.00[j]	170	−0.93[i]	5.71	1.52

[a] In V versus SCE. [b] Uncertainty ±0.05 V. [c] In mV. [d] In eV, computed using B3LYP and extended ECP basis sets. [e] In 0.1 M $BuNClO_4$/MeCN. [f] From ref 42a, measured by polarography at a dropping mercury electrode. [g] From ref 42b, measured by second harmonic alternating current voltammetry at a gold electrode. [h] Experimental data from NIST Standard Reference Database. [i] In 0.1 M Bu_4NClO_4/DMSO. [j] In 0.3 M Bu_4NBF_4/THF. [k] Uncertain value because of experimental difficulties.

Table 2. Computed Molecular Properties of the Center Atom (M) of $R_3M^{\bullet}$, R_3M^+, and R_3M^-

	Geometry[a]				Charge[c]		
	radical	cation	anion	spin density[b]	radical	cation	anion
$Ph_3C^{\bullet}$	1.473	1.457	1.463	0.59	0.04	0.18	−0.07
	120	*120*	*120*		*−0.87*	*−0.62*	*−1.37*
$Ph_3Si^{\bullet}$	1.866	1.814	1.929	0.82	0.35	0.76	−0.06
	114.3	*120*	*102.9*		*−0.39*	*0.36*	*−1.34*
$Ph_3Ge^{\bullet}$	1.966	1.902	2.053	0.80	0.13	0.49	−0.19
	112.0	*120*	*98.6*		*−0.25*	*0.51*	*−1.22*
$Ph_3Sn^{\bullet}$	2.153	2.081	2.251	0.77	0.43	0.88	0.04
	109.1	*120*	*95.3*		*−0.03*	*0.93*	*−1.22*
$Bu_3Sn^{\bullet}$	2.188	2.135	2.271	0.83	0.60	1.00	0.21
	107.5	*120*	*95.0*		*0.08*	*1.21*	*−1.17*

[a] Computed using B3LYP and extended ECP basis sets; optimized C−M bond lengths are in angstroms and C−M−C angles in degrees (shown in italics). [b] Computed M atom spin density using Mulliken population analysis. [c] Computed M atom charges using Mulliken population analysis and the CHELPG approach (shown in italics).

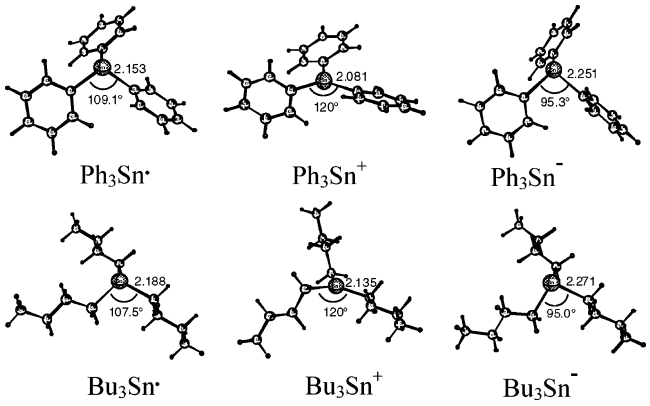

Figure 4. Geometries of $R_3Sn^{\bullet}$, R_3Sn^+, and R_3Sn^- optimized using B3LYP and extended ECP basis sets.

sum of the C and M covalent radii,[47] pointing to the presence of resonance interactions. However, the computed charges indicate that the resonance-donation to the center decreases significantly when going down the periodic table, and both approaches suggest that Ph_3Sn^+ has a center charge of around 0.9 while for Ph_3C^+ it is much less positive. The CHELPG approach even finds a large negative charge on the central C atom in Ph_3C^+. The difference in geometry and charge distribution between Bu_3Sn^+ and Ph_3Sn^+ is relatively small, which confirms that resonance interactions are not particularly significant in the latter case.

The geometrical features of the Ph_3C^- series are similar to those of the $Ph_3M^{\bullet}$ series, in that Ph_3C^- has a planar center while the heavier anions are pyramidal. On the other hand, the C−M−C angles are generally smaller and the C−M bond lengths longer for the anions than for the radicals. These observations indicate, not surprisingly, that the resonance interactions in Ph_3M^- are weaker than those in $Ph_3M^{\bullet}$. Both the Mulliken and the CHELPG approaches find small differences in the charge of the central atom when going down the periodic table. However, while Mulliken population analysis predicts the central atom to be near neutral, the CHELPG approach gives a strongly negative center. The geometry around the center atom as well as the charge is similar for Bu_3Sn^- and Ph_3Sn^-. This supports the notion that resonance stabilization in Ph_3Sn^- is relatively small.

Ionization Potentials and Electron Affinities. Computed ionization potentials (IP) and electron affinities (EA) are included in Table 1. Unfortunately, it is difficult to estimate the reliability of these values because of the lack of experimental data. The only data we have found for the $Ph_3M^{\bullet}$ series is the EA of $Ph_3C^{\bullet}$, which has been measured to be 1.56 ± 0.10 eV.[48] This is in relatively good agreement with our computed value of 1.43 eV. As a test of our computational approach, we calculated the IP and EA for the related $PhCH_2^{\bullet}$. The computed and experimental IP values are 7.09 and 7.24 eV, respectively. The corresponding EA values are 0.80 and 0.91 eV, respectively. Thus, our comparisons with experiment indicate that the average error in the computed IPs and EAs is close to 0.15 eV. This is also in agreement with the expected accuracy of the B3LYP method from testing on the extended G2 set[49] and from our previous calculations on arylthiyl and arylselanyl radicals.[11,12] It should be noted that the present study contains compounds with heavier elements than in previous studies, and thus it is possible that the accuracy in these cases is slightly lower.

The IP of 5.88 eV obtained for $Ph_3C^{\bullet}$ is significantly larger than the IP of 5.45 eV for $Ph_3Si^{\bullet}$. This may be attributed to the larger resonance stabilization of the former radical as indicated by the fact that $Ph_3C^{\bullet}$ has a planar center, whereas $Ph_3Si^{\bullet}$ is pyramidal. There is a relatively small but systematic increase in IP along the series $Ph_3Si^{\bullet}$, $Ph_3Ge^{\bullet}$, and $Ph_3Sn^{\bullet}$, which can be seen as an effect of a decreasing resonance stabilization of the corresponding cations for the heavier elements. In general, the effect of the center atom thus appears to be rather modest on the IPs. Moreover, the difference between the IPs for $Bu_3Sn^{\bullet}$

(47) The bond lengths of C−C, C−Si, C−Ge, and C−Sn, as estimated from the covalent radii (Cotton, F. A.; Wilkinson, G.; Gaus, P. L. *Basic Inorganic Chemistry*; Wiley: New York, 1987), are 1.54, 1.94, 1.99, and 2.17 Å, respectively.

(48) NIST Standard Reference Database No. 69.

(49) Curtiss, L. A.; Raghavachari, K.; Redfern, P. C.; Pople, J. A. *J. Chem. Phys.* **2000**, *112*, 7374.

and $Ph_3Sn^•$ is only 0.04 eV, showing that the effect of butyl and phenyl groups is similar.[50]

The EA generally increases going from $Ph_3C^•$ to $Ph_3Sn^•$. This is most likely an effect of the increasing charge capacity for the center atom along this series. The charge capacity refers to the ability of an atom or group to accept or donate charge.[51] Consideration of charge capacity has allowed the explanation of a number of seemingly anomalous aspects of chemical behavior,[52] such as the low EA of the fluorine atom and that the gas-phase acidity of fluoroacetic acid is lower than that of chloroacetic acid. However, resonance stabilization may also play a certain role, as the EAs of $Ph_3C^•$ and $Ph_3Si^•$ are almost identical despite the fact that Si has a significantly higher charge capacity. As discussed above, resonance stabilization is larger for Ph_3C^- than for Ph_3Sn^-. In a similar manner, resonance stabilization of the anion might, in principle, explain why the EA of $Ph_3Sn^•$ is 0.56 eV larger than that of $Bu_3Sn^•$, although the fact that the phenyl group in contrast to the butyl group is an inductive electron acceptor should be considered, as well. In other words, there seems to be a comparatively large group effect on EA.

Returning now to the measured potentials for $Ph_3C^•$ in Table 1, we have a better basis for understanding that the order is Sn > Ge > C > Si with respect to the reduction potentials and C > Si for the two oxidation potentials. From a qualitative point of view, it would be expected that $Ph_3C^•$ with the central C atom having an electronegativity of 2.5 should be the radical relatively hardest to oxidize and easiest to reduce. In comparison, the electronegativities of Sn, Ge, and Si are all in the range of 1.7−1.8. However, the effect from the higher charge capacity of Ge and Sn also comes through and provides an explanation for the less negative values of $E^{red}_{1/2}$ for $Ph_3Ge^•$ and $Ph_3Sn^•$ compared to that for $Ph_3C^•$. Moreover, the relatively strong delocalization present for the planar $Ph_3C^•$ in contrast to the other pyramidal radicals will tend to make the redox potentials of $Ph_3C^•$ more extreme, that is, shift the $E^{ox}_{1/2}$ and $E^{red}_{1/2}$ values in positive and negative directions, respectively.[53] The change observed in $E^{red}_{1/2}$ upon replacing the phenyl groups in $R_3Sn^•$ by butyl groups constitutes −490 mV in THF and −390 mV in DMSO. This is mainly due to delocalization and, in particular, inductive effects for Ph_3Sn^- as discussed for the EA values above. Note that the group effect amounts to as much as 700 mV[17] when the center atom is C due to its smaller charge capacity. One final important factor influencing the values of $E^{red}_{1/2}$ and $E^{ox}_{1/2}$ is the solvation of the species involved. The solvation energies constitute the main difference between the redox potentials and the corresponding gas-phase parameters, EA and IP. In the next section, this issue will be our main concern.

Table 3. Differentiated Solvation Energies, $\Delta\Delta G^o_{Sol}(+•)_{exp}$ and $\Delta\Delta G^o_{Sol}(-•)_{exp}$, Obtained for $R_3M^•$ in MeCN from Experimental Solution Data and Computed Gas-Phase Data along with Computed Differentiated Solvation Energies, $\Delta\Delta G^o_{Sol}(+•)_{PCM}$ and $\Delta\Delta G^o_{Sol}(-•)_{PCM}$

	$\Delta\Delta G^o_{Sol}(+•)_{exp}$[a,b]	$\Delta\Delta G^o_{Sol}(+•)_{PCM}$[a,c]	$\Delta\Delta G^o_{Sol}(-•)_{exp}$[a,b]	$\Delta\Delta G^o_{Sol}(-•)_{PCM}$[a,c]
$Ph_3C^•$	−20	−30.0	−54 (−51)[d]	−40.8
$Ph_3Si^•$	−26	−31.7	−44	−40.6
$Ph_3Ge^•$		−31.9	−55[e]	−38.6
$Ph_3Sn^•$		−32.8	−51	−38.0
$Bu_3Sn^•$	(−18)[f]	*g*	−48	*g*

[a] In kcal mol^{-1}. [b] Uncertainty ±5 kcal mol^{-1}. [c] Computed using B3LYP and extended ECP basis sets. [d] Computed from the experimental EA. [e] In DMSO. [f] Uncertain value because of experimental difficulties. [g] Values could not be obtained because of numerical problems in the PCM calculations.

Solvation Energies. The extraction of solvation energies based on the experimentally obtained redox potentials can be accomplished[54,55] through the use of eqs 8 and 9, as described in our previous work.[9−12]

$$\Delta\Delta G^o_{sol}(+•)_{exp} \equiv \Delta G^o_{sol}(+)_{exp} - \Delta G^o_{sol}(•)_{exp} = -IP + FE^o_{R_3M^+/R_3M^•} + C \quad (8)$$

$$\Delta\Delta G^o_{sol}(-•)_{exp} \equiv \Delta G^o_{sol}(-)_{exp} - \Delta G^o_{sol}(•)_{exp} = EA - FE^o_{R_3M^•/R_3M^-} - C \quad (9)$$

The parameters, $\Delta G^o_{sol}(+)$, $\Delta G^o_{sol}(-)$, and $\Delta G^o_{sol}(•)$, denote the solvation energies of the cations, anions, and radicals, respectively. Without comparison, the major contributions to $\Delta\Delta G^o_{sol}(+•)$ and $\Delta\Delta G^o_{sol}(-•)$ will originate from the $\Delta G^o_{sol}(+)$ and $\Delta G^o_{sol}(-)$ terms because of the strong solvation of charges.[56] The potentials entered in these expressions are the values of $E^{ox}_{1/2}$ and either $E^o_{R_3M^•/R_3M^-}$ or $E^{red}_{1/2}$ obtained in acetonitrile, with the value of $E^o_{Ph_3Ge^•/Ph_3Ge^-}$ pertaining to DMSO presenting the only exception. The use of $E^{ox}_{1/2}$ and $E^{red}_{1/2}$ imposes an additional uncertainty in the extracted numbers because their thermodynamic significance is not well-defined. Still, the coherence between the results obtained with the PMV and LSV techniques justifies the inclusion of these potentials in the calculations. For the constant *C*, a number of 109.3 kcal mol^{-1} is used, which originates from the value of the absolute potential of the standard calomel electrode (−4.74 V).[57,58]

In Table 3, the experimentally based solvation data, $\Delta\Delta G^o_{sol}(+•)_{exp}$ and $\Delta\Delta G^o_{sol}(-•)_{exp}$, are collected along with the corresponding computed values, $\Delta\Delta G^o_{sol}(+•)_{PCM}$ and $\Delta\Delta G^o_{sol}(-•)_{PCM}$, obtained from the PCM approach, as described in the Theoretical Approach section. When first the solvation energies of the anions is considered, it may be noted that the two sets of $\Delta\Delta G^o_{sol}(-•)$ values lie between −55 and −38 kcal mol^{-1}. This relatively strong solvation is indicative of a rather localized negative charge, which is consistent with a pyramidal geometry around the center atom in the anions. Still, $\Delta\Delta G^o_{sol}(-•)_{exp}$ is consistently found to be more negative than $\Delta\Delta G^o_{sol}(-•)_{PCM}$. Presumably, this should be attributed to

(50) Although this result cannot be related to oxidation potentials for any of the present systems, it might be mentioned that quite similar values are obtained for the two carbon-centered radicals, $Me_3C^•$ ($E^{ox}_{1/2}$ = 0.09 V versus SCE)[13b] and $Ph_3C^•$ ($E^{ox}_{1/2}$ = 0.27 V versus SCE).[42a]

(51) Huheey, J. E. *J. Phys. Chem.* **1965**, *69*, 3284. (b) Huheey, J. E.; Watts, J. C. *Inorg. Chem.* **1971**, *10*, 1553. (c) Politzer, P. J. *Chem. Phys.* **1987**, *86*, 1072.

(52) Politzer, P.; Huheey, J. E.; Murray, J. S.; Grodzicki, M. *J. Mol. Struct. (THEOCHEM)* **1992**, *259*, 99. (b) Brinck, T.; Murray, J. S.; Politzer, P. *Inorg. Chem.* **1993**, *32*, 2622.

(53) For a discussion of radical stabilities, see also: (a) Bordwell, F. G.; Bausch, M. J. *J. Am. Chem. Soc.* **1986**, *108*, 1979. (b) Bordwell, F. G.; Cheng, J.-P.; Ji, G.-Z.; Satish, A. V.; Zhang, X.-M. *J. Am. Chem. Soc.* **1991**, *113*, 9790. (c) Bordwell, F. G.; Zhang, X.-M.; Alnajjar, M. S. *J. Am. Chem. Soc.* **1992**, *114*, 7623.

(54) Matsen, F. A. *J. Chem. Phys.* **1956**, *24*, 602.

(55) Peover, M. E. *Trans. Faraday Soc.* **1962**, *58*, 1656.

(56) The use of IP and EA in these equations is based on the approximation that they are equal to the corresponding Gibbs energy entities.

(57) Reiss, H.; Heller, A. *J. Phys. Chem.* **1985**, *89*, 4207.

(58) Lim, C.; Bashford, D.; Karplus, M. *J. Phys. Chem.* **1991**, *95*, 5610.

the fact that we were forced to use a larger scale factor than recommended for the cavity generation in the PCM calculations, leading to an increase in $\Delta\Delta G^{o}_{sol}(-\bullet)_{PCM}$ by around 2−4 kcal mol^{-1}. In addition, the recommended scale factor has been optimized for neutral molecules, and calculations on anions are often found to give too positive solvation energies. Furthermore, the scale factor is optimized for Hartree−Fock wave functions which generally give more polarized charge distributions and thus more negative solvation energies. Considering such effects, it is not unlikely that $\Delta\Delta G^{o}_{sol}(-\bullet)_{PCM}$ is overestimated by 6−8 kcal mol^{-1}, which would put the computed values in better agreement with the experimental ones. Still, some noteworthy exceptions remain. For instance, $\Delta\Delta G^{o}_{sol}(-\bullet)_{exp}$ for Ph_3C^- is 13 kcal mol^{-1} more negative than the $\Delta\Delta G^{o}_{sol}(-\bullet)_{PCM}$ value. The difference is reduced to 10 kcal mol^{-1} if the experimental rather than the computational EA is used to calculate $\Delta\Delta G^{o}_{sol}(-\bullet)_{exp}$. A plausible explanation for the remaining difference between the two values could be that there is a difference between the gas phase and solution geometry. The gas-phase geometry optimization shows that Ph_3C^- in contrast to the other anions is planar around the center atom. However, a pyramidal center will give a more localized charge and therefore a more negative solvation energy. Thus, it is possible that a pyramidal geometry for Ph_3C^- is favored in solution. Also for Ph_3Sn^-, there is a relatively large difference between $\Delta\Delta G^{o}_{sol}(-\bullet)_{PCM}$ and $\Delta\Delta G^{o}_{sol}(-\bullet)_{exp}$. Furthermore, it is surprising that $\Delta\Delta G^{o}_{sol}(-\bullet)_{exp}$ for Ph_3Sn^- is 7 kcal mol^{-1} more negative than that for Ph_3Si^- since both are pyramidal and since the larger size of Sn should lead to a less effective solvation. In this case, we speculate that the accuracy in the computed EA of $Ph_3Sn^\bullet$ or $Ph_3Si^\bullet$ may be too low for an accurate prediction of the solvation energy. The solvation energies of Ph_3Sn^- and Bu_3Sn^- are almost equal as expected on account of the rather similar charges and geometries computed. For none of the anions studied, the solvation is strong enough to indicate the presence of any covalent or charge-transfer interactions with the solvent. This result is in line with the observation that the solvent effect on the reduction potentials for $Ph_3Sn^\bullet$ and $Bu_3Sn^\bullet$ constitutes less than 190 mV. If strong interactions existed between the anions and the solvent, much larger differences would have been expected.

The two sets of $\Delta\Delta G^{o}_{sol}(+\bullet)$ values are in the range from −33 to −20 kcal mol^{-1}. These values are significantly less negative than the corresponding $\Delta\Delta G^{o}_{sol}(-\bullet)$ numbers, which is expected in the sense that the planar geometry around the center atom for Ph_3M^+ leads to more spread out charge than for a pyramidal geometry and accordingly to a weaker solvation. At the same time, this also indicates that there is no strong covalent interaction present with the solvent for these kinds of cations in contrast to arylsulfenium[10,11] and arylselanylium ions[12] in MeCN. However, it is surprising that $\Delta\Delta G^{o}_{sol}(+\bullet)_{PCM}$ is more negative than $\Delta\Delta G^{o}_{sol}(+\bullet)_{exp}$. Because of the too-large scale factor employed in the PCM calculation, we would rather have anticipated the opposite order. This seems to suggest that the discrepancy between experiment and theory, at least partly, should be attributed to errors in the computed IP and/or the experimental oxidation potentials. It is interesting to note that both computations and experiments predict a more negative solvation energy for Ph_3Si^+ than for Ph_3C^+, despite the fact that carbon is the smaller atom. This could be attributed to the more positive charge on the center atom in Ph_3Si^+, as found by both the Mulliken and the CHELPG approaches. In fact, the PCM method predicts a consistent decrease in $\Delta\Delta G^{o}_{sol}(+\bullet)_{PCM}$ going from Ph_3C^+ to Ph_3Sn^+, in agreement with the computed change in charge distribution using the CHELPG method.

Finally, some summarizing comments on the PCM approach seem appropriate. In a series of articles dealing with different organic cations and anions,[9,11,12] we have analyzed its performance in the computation of solvation energies. First of all, we find that the accuracy differs greatly for different types of molecules. The reason for this behavior can be attributed to the great dependence of the solvation energy on the cavity size found for PCM and other solvation methods based on dielectric continuum theory. In general, the accuracy can be increased by using specially optimized parameters that determine the size and shape of the cavity based on the hybridization and chemical environment of the atoms in the investigated compounds.[59] However, when studying novel molecules, such optimized parameters are seldom available or applicable. The present analysis shows that the average error in the computed solvation energy may for some sets of compounds be as high as 10 kcal mol^{-1} when using standard cavity parameters based on regular van der Waals radii. On the other hand, in our studies of parasubstituted thiophenoxides and phenylselenoates, experimentally and theoretically based solvation energies agreed within 2−4 kcal mol^{-1}.[11,12] The average errors on the substituent effects on the solvation energies were even lower. These results are remarkably good considering the expected errors of a few kcal mol^{-1} in the experimental solvation energies and show that a relatively high accuracy can be expected of the PCM approach for analysis of substituent effects. We have also found that when experimentally determined solvation energies are considerably more negative than the PCM results, this can often be attributed to strong specific interactions present between the solvent and solute. This was demonstrated for the solvation of arylsulfenium and arylselanylium ions in MeCN, where covalently bonded adducts were identified by theoretical calculations.[11,12] In such cases, we have shown that accurate solvation energies can be obtained by using the PCM method in a supermolecular approach, where the important solvent molecules are explicitly considered in the calculations.

Conclusions

Redox potentials of a number of triphenyl- or tributyl-substituted Si-, Ge-, or Sn-centered radicals, $R_3M^\bullet$, have been measured in acetonitrile, tetrahydrofuran, or dimethyl sulfoxide by photomodulated voltammetry or through a study of the oxidation process of the corresponding anions in linear sweep voltammetry. The combined results provide the ranges of potentials in which to expect radical and ion chemistry. This information is of great importance in the understanding and control of polymerization processes involving such species. For the reduction potentials determined in more than one solvent, the variation is less than 190 mV. As far as the effect exerted by the different group IV elements on the data obtained for the $Ph_3M^\bullet$ series is concerned (including literature results for M = C), the order of reduction potentials follows Sn > Ge > C > Si, while for the two oxidation potentials, it is C > Si. As to

(59) Barone, V.; Cossi, M.; Tomasi, J. *J. Chem. Phys.* **1997**, *107*, 3210.

the substituent effect of the R group in $R_3Sn^{\bullet}$, the reduction potential is more negative by 490 mV in tetrahydrofuran (390 mV in dimethyl sulfoxide) when R is a butyl rather than a phenyl group. These trends can be explained qualitatively through a combination of effects, such as charge capacity being most pronounced for the heavier elements, resonance stabilization present for the planar $Ph_3C^{\bullet}$ and all R_3M^+, and finally a contribution from solvation as supported by quantum-chemical calculations. The solvation is found to be stronger for R_3M^- than for R_3M^+, indicating that no covalent interaction exists between the cations and the solvent as observed for arylsulfenium and arylselanylium ions in acetonitrile. The relatively strong solvation of R_3M^- is attributed to the presence of a rather localized negative charge in the pyramidal geometry, while the planar geometry around the center atom in R_3M^+ leads to more spread out charge and a weaker solvation. Calculated solvation energies based on the PCM approach can reveal these trends roughly, but they are not able to reproduce the experimentally derived values on a detailed level for these types of ions.

Acknowledgment. Statens Naturvidenskabelige Forskningsråd and Torkil Holms Fond are thanked for financial support.

Supporting Information Available: Tables of absolute energies and Cartesian coordinates, along with a figure of the optimized geometries of $R_3M^{\bullet}$, R_3M^+, and R_3M^-. This material is available free of charge via the Internet at http://pubs.acs.org.

JA044687P